Hindawi Publishing Corporation
Shock and Vibration
Volume 2016, Article ID 2959763, 10 pages
http://dx.doi.org/10.1155/2016/2959763

Research Article

Performance Analysis of a Magnetorheological Damper with Energy Harvesting Ability

Guoliang Hu,[1,2] Yun Lu,[2] Shuaishuai Sun,[2] and Weihua Li[2]

[1]*Key Laboratory of Conveyance and Equipment, The Ministry of Education, East China Jiaotong University, Nanchang, Jiangxi 330013, China*
[2]*School of Mechanical, Materials and Mechatronic Engineering, University of Wollongong, Wollongong, NSW 2522, Australia*

Correspondence should be addressed to Guoliang Hu; glhu2006@163.com and Weihua Li; weihuali@uow.edu.au

Received 18 May 2016; Accepted 11 July 2016

Academic Editor: Londono Monsalve

A magnetorheological (MR) damper with energy harvesting ability was proposed based on electromagnetic induction (EMI) principle. The energy harvesting part was composed of a permanent magnet array and inducing coils which move vertically. This device could act as a linear power generator when the external excitation was applied, and the kinetic energy could be converted into electrical energy due to the relative linear motion between the magnets array and the inducing coils. Finite element models of both the MR damper part and the linear power generator part were built up separately to address the magnetic flux distributions, the magnetic flux densities, and the power generating efficiency using ANSYS software. The experimental tests were carried out to evaluate the damping performance and power generating efficiency. The results show that the proposed MR damper can produce approximately 750 N damping forces at the current of 0.6 A, and the energy harvesting device can generate about 1.0 V DC voltage at 0.06 m·s^{-1} excitation.

1. Introduction

Over the past couple of decades, magnetorheological (MR) fluid has undergone significant development due to its unique rheological properties under exerted magnetic fields [1]. These features have led to the development of many MRF-based devices such as the MR damper, MR valve, MR brake, and MR clutch. The most popular MRF-based devices are MR dampers due to their long range controllable damping force, fast adjustable response, and low energy consumption [2].

Till now, the MR dampers have wide applications in automotive industry including off-road vehicles [3, 4], and they are also used in naval gun controlling [5], field of landing gear [6], prosthetic knees [7], washing machines [8], high speed train suspension [9, 10], seismic vibration control of different civil structures [11, 12], and so forth. However, a significant drawback of traditional MR damper is witnessed; that is, the kinetic energy from the vibration is wasted in heating rather than harvested as a reusable power resource due to lack of energy harvesting device.

Recently, energy harvesting MR dampers have received a great deal of attention due to their capability of recovering kinetic energy that normally dissipated by traditional MR dampers. Many researchers explored different principles and designs of energy harvesting MR dampers, which can be classified into two main categories. The first category is to convert the linear damper vibration into oscillatory rotation and use rotational permanent magnetic DC or AC generators to harvest kinetic energy. These mechanical mechanisms include rack and pinion, ball screw, and hydraulic transmission. Avadhany et al. [13] patented one type of rotary regenerative shock absorber based on hydraulic transmission. Choi et al. [14] proposed an electrorheological (ER) shock absorber integrated with a generator by employing a rack and pinion gear mechanism, which converted a linear motion of the piston to a rotary motion, thus activating a generator to produce electrical energy to self-power the excitation coil in the piston head. Li and Zuo [15, 16] proposed an energy harvesting shock absorber with a mechanical motion rectifier (MMR), the roller clutches were embedded in two bevel

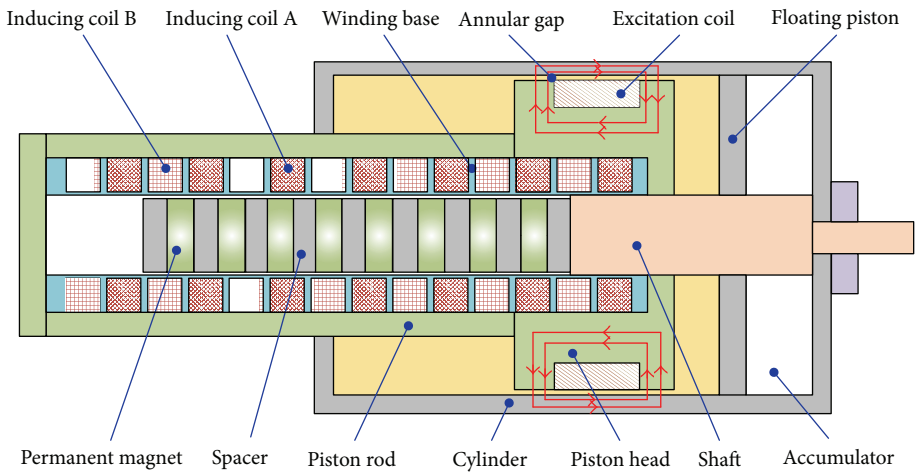

Figure 1: Schematic diagram of the proposed MR damper with energy harvesting ability.

gears, and the function of "motion rectifier" was achieved with three bevel gears in the MMR. Yu et al. [17] proposed a new type of energy harvesting device system for the wireless sensing of inner-state conditions in the operation of MR dampers, where an impeller mechanism was used as the amplitude convert device, and an AC generator was applied as the energy converting part to convert the linear shock into electrical energy. Zhang et al. [18] developed and prototyped a regenerative shock absorber based on a ball screw mechanism and validated it with full vehicle experiments in the lab. Guan et al. [19] proposed a novel MR damper with a self-powered capability; the vibration energy harvesting mechanisms were adopted based on ball screw mechanisms and a rotary permanent magnet DC generator, which converted the external vibration energy into electrical energy to power the MR damping unit.

In addition to the energy harvesting with mechanical transmission mechanism in the MR damper, the second category is based on the design of an electromagnetic induction (EMI) device, which generates power from the relative linear motion between magnets and coils. Cho et al. [20] proposed a special structure of an EMI device to be used with an MR damper. Choi et al. [21] investigated experimentally a smart passive control system comprising an MR damper and an EMI device to generate electrical power. Choi and Wereley [22] studied the feasibility and effectiveness of a self-powered MR damper using a spring-mass EMI device. Sapiński established a permanent magnet power generator for MR damper, the designed vibration generator consisted of a special arrangement and a foil wound coil, and the numerical analysis and experiment were carried out to investigate the magnetic field distribution and efficiency of the generator [23, 24]. Then, Sapiński proposed a multipole magnetic generator, the design of permanent magnets array was optimized, and both numerical method and finite element simulation were carried out to investigate the performance of the whole energy harvesting MR damper [25]. However, the large cogging force generated in the interaction between ferromagnetic components and permanent magnets array led to a negative impact on the control of MR damper. Chen and Liao also proposed a self-sensing MR damper with power generation; the design of the power generator significantly minimized the cogging force and improved the dynamic damping performance [26]. The guild layer and shield layer were adopted to minimize magnetic interaction effect between permanent generator and MR damper. However, the extra shield and guild layer increased the complex of the whole structure while the component itself provided litter contribution to the dynamic control or improvement of generating effect.

In this paper, a new MR damper with energy harvesting ability was proposed based on the EMI principle. The sharing component between the damper part and the linear power generator part could minimize the magnetic field interference without extra guild layer and shell layer; also the component itself provided necessary function in both generating process and damping capability. This new design is expected to simplify the structure of linear power generator and also provided a low cogging force. The inducing coils in the linear power generator had two representative electric circuits. In this study, finite element method was utilized to address the magnetic field distribution and magnetic flux density for the damper part and linear power generator part, respectively, and cogging force conducted from linear power generator was also identified. The properties of proposed MR damper were experimentally investigated, and power regenerative characteristics were also discussed.

2. Principle and Structure of the Proposed MR Damper with Energy Harvesting Ability

Figure 1 shows the schematic diagram of the proposed MR damper with energy harvesting ability. The MR damper consists of a damping part and a linear power generator part. In the damping part, there are two chambers in the cylinder, and the chamber is separated by a floating piston. The chamber with piston is filled with MR fluid, and the other chamber is used as an accumulator to compensate the

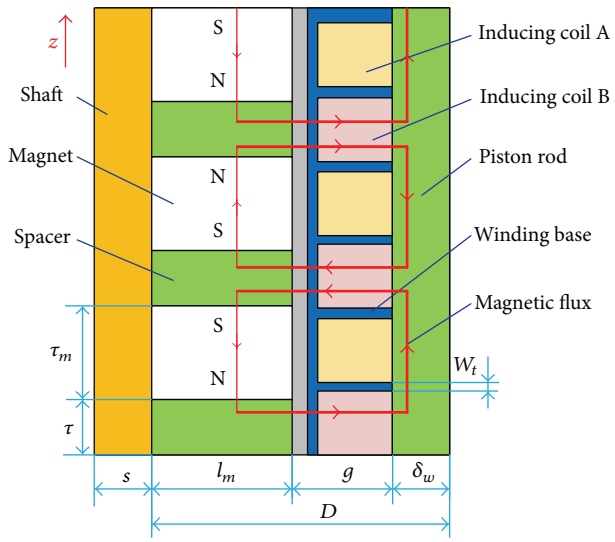

Figure 2: Magnetic circuit of the linear power generator.

volume change when the piston rod moves vertically along the vibration direction. A compression spring is stalled in the accumulator to support the movement of floating piston. When the piston rod moves, the MR fluid in the cylinder flows through the annular gap between piton head and cylinder. The excitation coil wound around the piston head is electrically insulated. When a direct current was applied on the excitation coil, a magnetic field is generated around the excitation coil and piston head. Then the annular gap would become an activated area and the viscosity of MR fluid in the gap would be changed. Finally, the changeable damping force is achieved.

The linear power generator is radially arranged inside the MR damper. Each two permanent magnets are separated by a spacer; also a magnet and a spacer are grouped to a pole pair. There are totally eight pairs of magnet-spacer assembling together, and they are screwed on the shaft. The inducing coil was arranged on the winding base. The phase of the generated voltage depends on the magnetic field distribution, the phase angle is 90° between each nearby coil, and each two different phases of coil are connected together to increase power generating efficiency. In this design, the 0° and 180° phase coils are connected together, which is called coil A; also the 90° and 270° are connected together, which is called coil B. Thus, the 14 phase coils are wound in the winding base and combined into two inducing coils, that is, coil A and coil B. When the interaction between permanent magnets and inducing coils occurred, the vibration energy would be converted into electrics into coil A and coil B.

The magnetic circuit of the linear power generator is shown in Figure 2. The rotor of the linear power generator consists of a winding base and two inducing coils A and B, and the stator is assembled by a shaft, permanent magnets, and spacers. Each pole pair includes a permanent magnet and a pole spacer, and 8 pairs of magnet arrays are installed on the shaft; and the shaft is fixed by the cylinder through the screw, and this structure is also called multipole. As shown in Figure 2, the magnetic flux radially passes through the half-length of the spacer and then through air gap and the inducing coil, reaching the piston rod, and then returns to the winding base, air gap, and half-length of spacer, finally reaching the opposite of permanent magnet.

3. Finite Element Analysis of the Proposed MR Damper with Energy Harvesting Ability

In order to address the magnetic field distribution and magnetic flux density on the piston head and the generating property of the linear power generator, the finite element models were built up using ANSYS software, and the issues of cogging force and magnetic interference were also discussed in this section.

3.1. Modelling of the MR Damper Part. As shown in Figure 1, the damper piston is radially outside of the linear power generator. The benefit of this structure is that the piston rod is utilized both as the shield and outer core of the linear power generator. This design can minimize the magnetic interaction between the linear power generator and the MR damper part while not adding extra structure in the damper. As the producer of electromagnetic field, the excitation coil is considered as electromagnet. By varying the driving current through the excitation coil, the magnetic flux density can be varied too. The DC current is supplied to the excitation coil, and the current density J_S is given by

$$J_S = \frac{NI}{A}, \tag{1}$$

where N is the number of turns of the excitation coil, I is the DC current, and A is the cross-sectional area of the coil.

In this simulation analysis, the physics environment is set as magnetic nodal option from preferences of ANSYS. The two-dimensional axisymmetric entity model of the MR damper part is built up as shown in Figure 3(a). The entity model includes the piston rod, the piston head, the excitation coil, the cylinder, and the resistance gap filled with MR fluid. Figure 3(b) presents the finite element model of the damper part. The element type is chosen as PLANE 13, and the 4-node quadrilateral meshing is used for the finite element model. This model is divided into 1237 elements and 3850 nodes. The leakage of magnetic flux is considered to acquire the reliable magnetic field distribution for the piston head.

Figure 4 illustrates the finite element model and static electromagnetic field simulation of the MR damper part. Figure 4(a) shows the magnetic flux of the MR damper part; it can be seen that the magnetic flux vertically passes through the annular gap, which means the high efficiency of magnetic field. Figure 4(b) illustrates the magnetic flux density of the main area for the MR damper part; the magnetic flux density within the annular gap ranged from 0.55 T to 0.74 T when the excitation current was set as 1 A, which leads to generating a large damping force.

Figure 5 shows the magnetic flux density of the annular resistance gap under the different applied current. As shown in the figure, the magnetic flux density is increased with

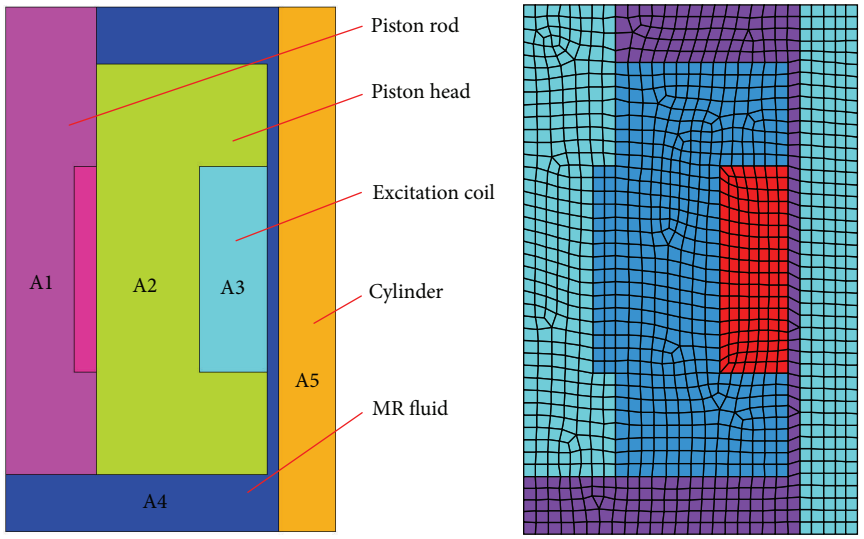

Figure 3: Modelling of the MR damper part: (a) entity model and (b) finite element model.

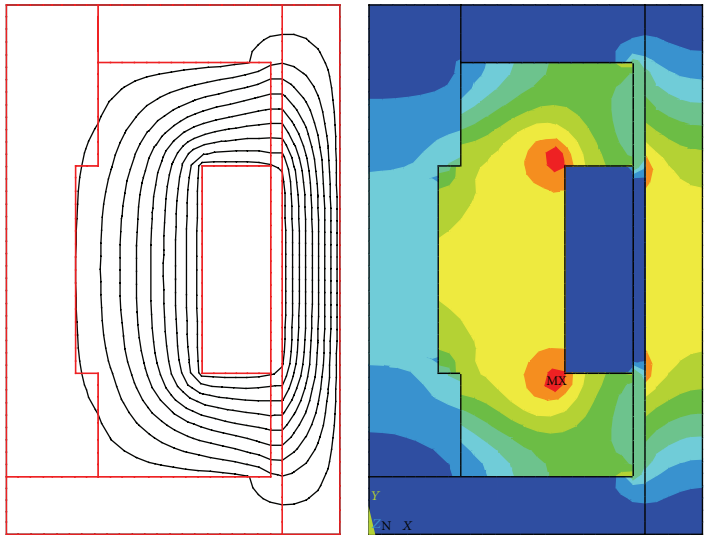

Figure 4: Finite element analysis of MR damper part: (a) magnetic flux distribution and (b) magnetic flux density.

the increment of the applied current. The most efficient energy utilization point occurred at the current of 0.6 A, and the magnetic saturation point occurred at the point of 1 A excitation.

Figure 6 shows the relation between damping force and displacement under different applied current. The amplitude is set as 5 mm and the frequency is 1 Hz. Observing the figure, the damping force increased as the increasing of the excitation, and the change of damping force agreed well with the simulation result for the magnetic field.

3.2. Modelling of the Linear Power Generator Part. The numerical analysis was carried out to address the magnetic property for only one pole pair. It can be assumed that the reluctance values of the pole spacer are neglected for their high magnetic permeability; thus the magnetic flux is given as [27]

$$\phi_g = \frac{B_{\text{rem}}\tau_m\mu_0 H_c A_c}{2gB_{\text{rem}} + \tau_m\mu_0 H_c A_c \left(A_g/A_m\right)}, \tag{2}$$

where ϕ_g is the magnetic flux of air gap without considering the leakage, μ_0 is the relative magnetic permeability and equals $4\pi \times 10e^{-7}$ (N/A^2), H_c is the magnetic field intensity of magnet, B_{rem} is the flux density of the magnet, A_g is

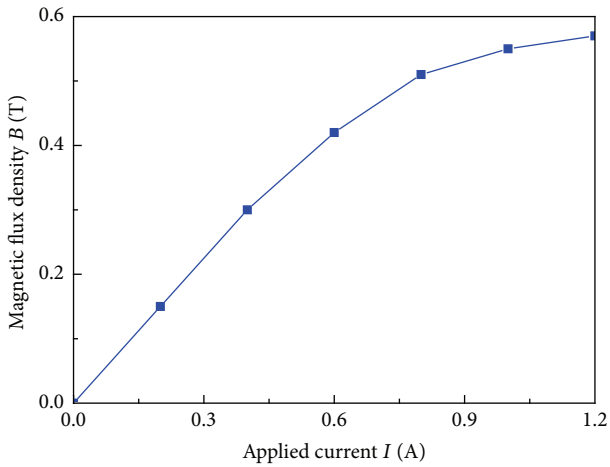

FIGURE 5: Magnetic flux density under different applied current.

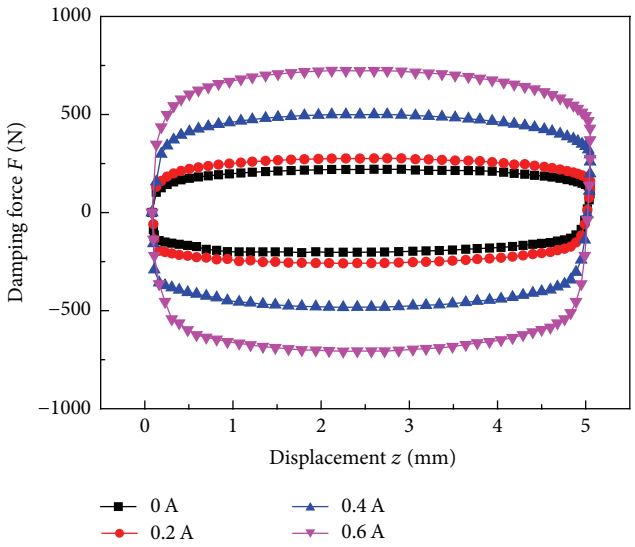

FIGURE 6: Damping force versus displacement at the different applied current.

the surface area of cylindrical air gap, A_m is the cross-section area of magnet, and A_g and A_m can be obtained by

$$A_g = \pi\left(s + l_m + \frac{g}{2}\right)\tau_m,$$
$$A_m = \pi\left[(s + l_m)^2 - s^2\right], \tag{3}$$

where s is the diameter of shaft, l_m is the thickness of the permanent magnet, g is the length of air gap between piston rod and permanent magnet array, and τ_m is the magnet thickness.

The induced voltage E in the inducing coil is defined as

$$E = -N\phi_g \frac{\pi}{\tau + \tau_m} \sin\left(\frac{\pi}{\tau + \tau_m} z + \theta\right)\frac{dz}{dt}, \tag{4}$$

where N is number of turns of the inducing coil, τ is spacer thickness, z is the displacement, dz/dt is the velocity, and θ is the initial phase angle of inducing coil.

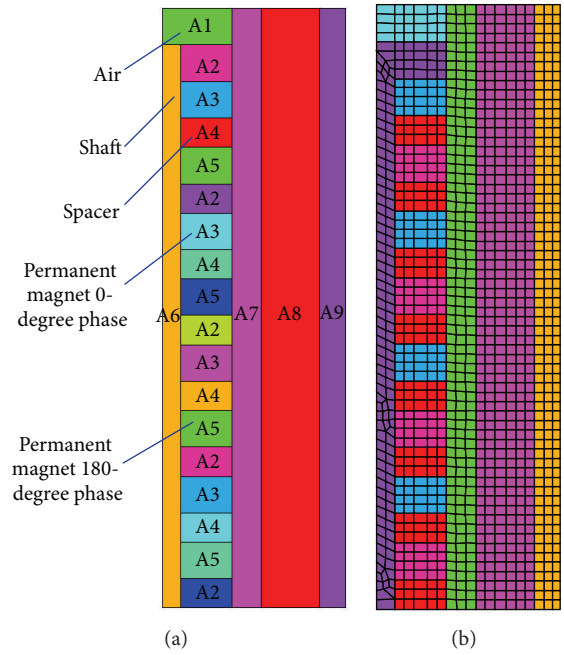

FIGURE 7: Modelling of the linear power generator: (a) entity model and (b) finite element model.

The number of turns of N is defined as

$$N = \frac{2A_c}{\sqrt{3}d^2}, \tag{5}$$

where A_c is the cross-sectional area of electrical wire and d is the diameter of the wire.

Figure 7 shows the modelling of the linear power regenerator. As shown in Figure 7(a), the main components of the linear power generator include the air chamber (A1), the permanent magnet arrays (A2, A3, A4, and A5), the shaft (A6), the winding base and inducing coils (A7), the piston rod (A8), and the zone filled with MR fluid (A9). There are two arrangements for the permanent magnets: 0° phase and 180° phase. Each two opposite arranged magnets are represented by a spacer. Figure 7(b) shows the finite element model of the linear power generator. The element type is chosen as PLANE 13, and the finite element model consists of 1217 elements and 3816 nodes. The winding base is made of ABS material, which is a nonmagnetic material; the electrical wire is made of brass material. As a result, the permeability of the two materials in the air gap is identical. The shaft is made of aluminum. The spacer and piston rod are made of steel 1020 which provide a high permeability.

Figure 8 illustrates the finite element analysis of the linear power regenerator. Figure 8(a) shows the magnetic flux distribution; the magnetic flux passes through the gap between the magnet arrays and the piston rod. As a result, the inducing coils installed in the winding base can generate induced voltage when the relative linear motion between the magnet arrays and inducing coil occurred. Figure 8(b) presents the static electromagnetic field distribution. The maximum magnetic flux density in the pole spacer is 0.9 T,

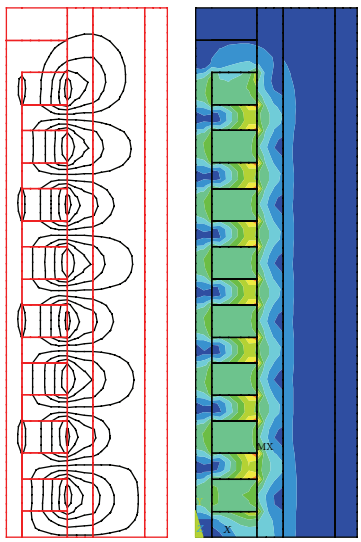

Figure 8: Finite element analysis of the linear power generator: (a) magnetic flux distribution and (b) magnetic flux density.

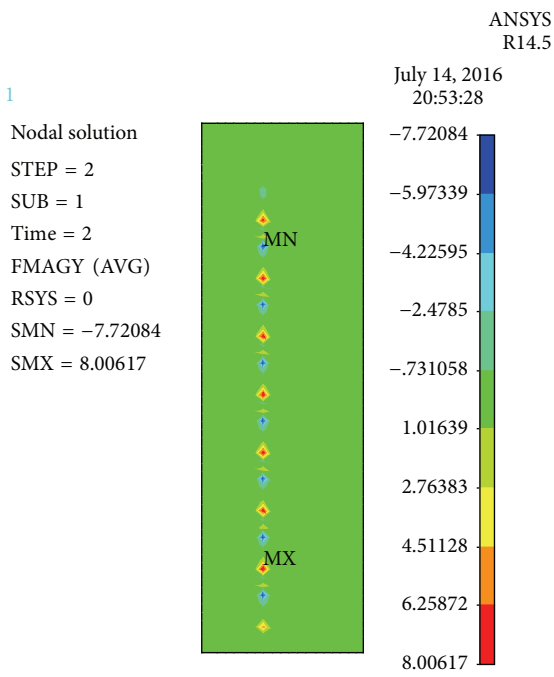

Figure 9: Magnet force distribution of the linear power generator.

while the flux density in the spacer is 0.3 T on average. The winding base is made of ABS material, which is a nonmagnetic material; also the electrical wire is made of brass material. As a result, the magnetic flux density within the inducing coils and the flux leakage coefficient is small.

Figure 9 shows the cogging force distribution of the linear power generator. As shown in the figure, a low cogging force is obtained due to the compact structural design, and the total cogging force is about 1 N.

Table 1: Specifications of the proposed MR damper.

Parameter	Value
Diameter of piston R	79 mm
Diameter of coil space R_c	50 mm
Thickness of cylinder R_h	5 mm
Gaps of MR fluid h	1 mm
Length of piston L	28 mm
Height of gallery W_c	9 mm
Length of gallery L_1, L_2	9 mm
Number of turns N	250
Weight of coil space L_c	18 mm
Diameter of excitation coil wire	0.5 mm
Resistance of excitation coil	4 Ω
Diameter of generator structure D	17 mm
Magnet thickness τ_m	5 mm
Magnet height l_m	5 mm
Magnet number	8
Diameter of rod s	2.5 mm
Spacer thickness τ	4 mm
Length of teeth W_t	2 mm
Thickness of piston rod δ_w	5 mm
Length of air gap g	4.5 mm
Coil maximum current	1.5 A
Coil wire turns	256
Diameter of inducing coil wire	0.5 mm
Resistance per inducing coil	4 Ω

4. Experiment Analysis of the Proposed MR Damper with Energy Harvesting Ability

4.1. Prototyping of the Proposed MR Damper. Figure 10 shows the main components and assembly of the manufactured MR damper, and the parameters of the MR damper are shown in Table 1. The cylinder and the piston rod are made of high magnetic material steel 1020, the shaft of the linear power generator is made of aluminum which is a nonmagnetic material, and the material used in spacers is steel 1020. The permanent magnets that are used in the design are NdFeB magnets grade N52. The magnets are stacked in pairs as shown in Figure 1; the magnetic flux passes through the spacers under the driving of opposite magnetomotive forces.

4.2. Damping Performance of the MR Damper Part. Figure 11 shows the damping properties under different coil currents, in the test, the frequency is set as 1 Hz and the amplitude is 5 mm, and the direct current is selected as 0 A, 0.2 A, 0.4 A, and 0.6 A, respectively. It can be seen that the damping force is about 200 N without the applied current; the reason is that the damping force at 0 A is generally from the stiffness of the accumulator and the MR fluid in the damper that works under Newtonian fluid model. The damping force increases from 200 N to about 750 N when 0.6 A current is applied. In this situation, the power consuming of the proposed damper is about 1.4 W. It can be seen that the damping force depends on the applied current, and the damping force will be changed

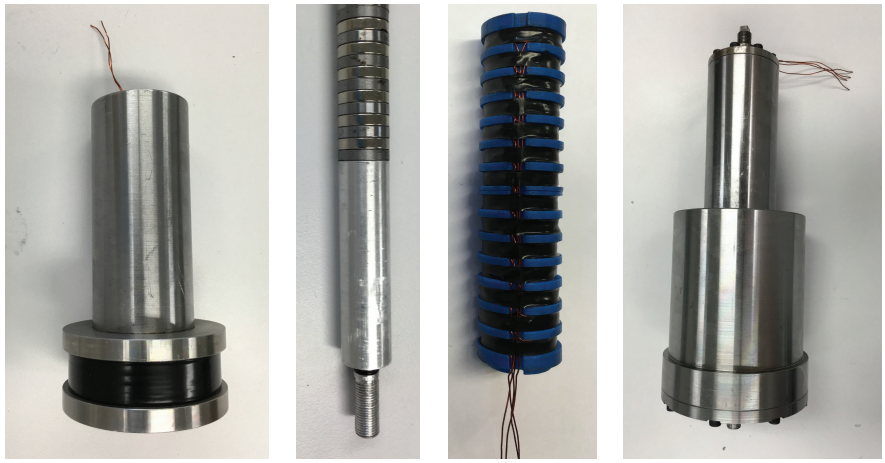

(a) (b) (c) (d)

Figure 10: The proposed MR damper: (a) piston head, (b) permanent magnets array and shaft, (c) winding base and inducing coils of generator, and (d) the assembly.

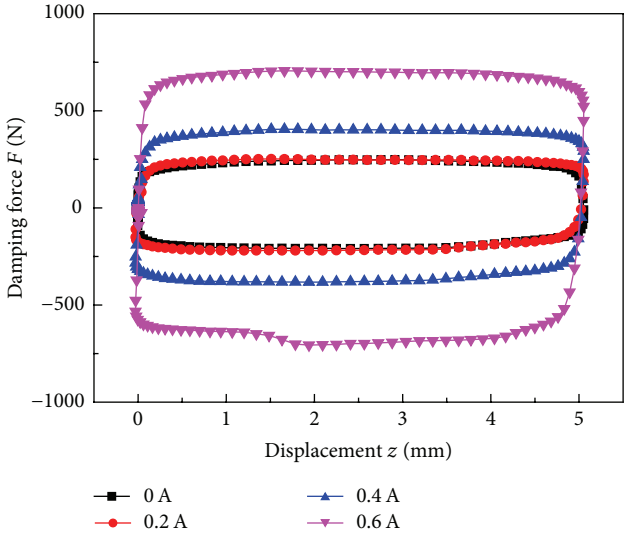

Figure 11: Damping force and displacement relation of the MR damper.

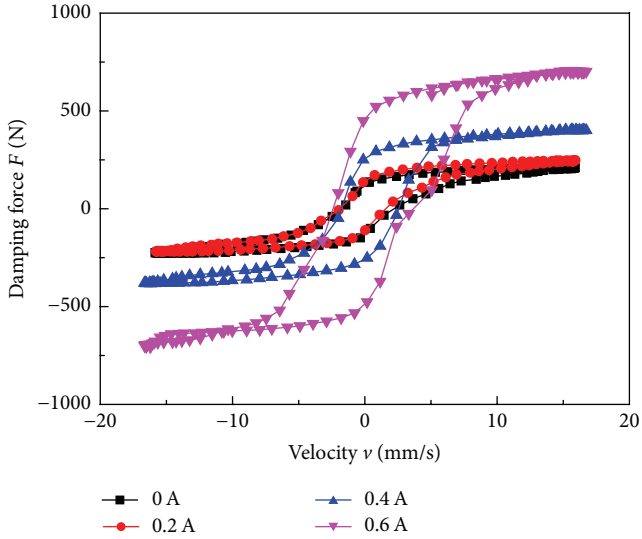

Figure 12: Damping force and velocity relation of the MR damper.

by changing the current input. Thus, the proposed damper could generate large controllable damping force output, while under relatively low power consumption.

Figure 12 illustrates the damping force and velocity response under different applied currents, and in the test, the frequency is set as 1 Hz and the amplitude is 5 mm. The maximum velocity is 17 mm/s when the MR damper operates under 0.6 A excitation.

Figure 13 shows the comparison of damping force between the theoretical result and experimental result. The excitation current is set at 0.6 A. As shown in Figures 13(a) and 13(b), the theoretical results agree well with the experimental ones. It can be summarized that the feasibility of proposed analysis had been proved.

4.3. Energy Harvesting Capability of the Linear Power Generator without AC-DC Rectifier. In this experiment, the measured inducing voltage from the two inducing coils A and B illustrated the properties of the linear power regenerator. The calculation data was obtained by the numerical analysis mentioned in Section 3.2. The comparison of inducing voltage between numerical analysis and experiment measurement is shown in Figure 14. Observing Figures 14(a) and 14(b), the experiment data from coil A and coil B agreed well with the numerical results, and the measured peak inducing voltage is 1.22 V. However, the wave of the inducing voltage is not the typical sinusoidal wave when the amplitude increases; the reason is the effect of frequency multiplication [26].

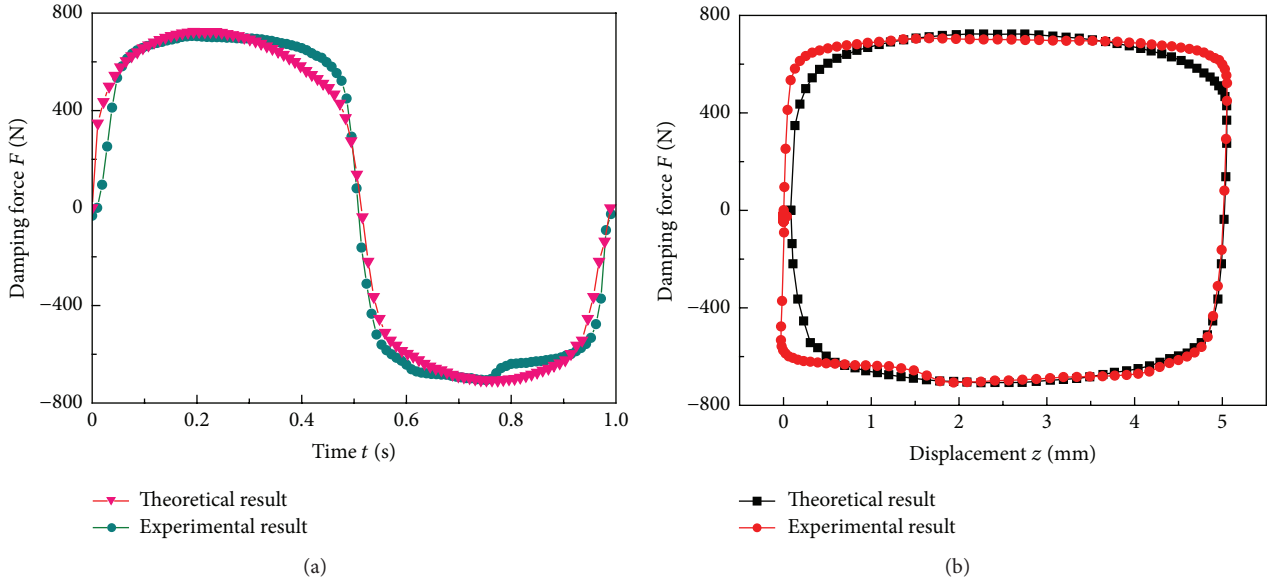

FIGURE 13: Comparison between theoretical result and experimental data: (a) damping force versus time and (b) damping force versus displacement.

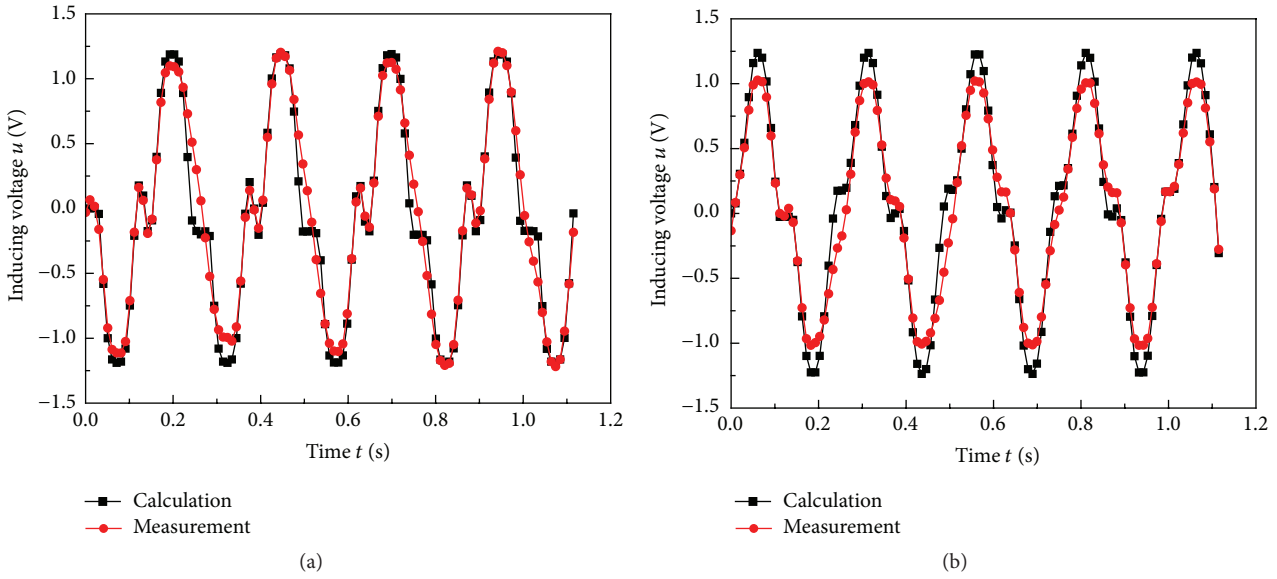

FIGURE 14: Comparison between numerical analysis result and experimental test of inducing voltage: (a) coil A and (b) coil B.

4.4. Energy Harvesting Capability of the Linear Power Generator with AC-DC Rectifier. Because the inducing coils installed in the piston are equivalent as an electrical inductance, the value of generated DC voltage is better to evaluate the performance effect of proposed linear power generator compared with AC voltage. Thus, a bridge rectifier is developed, and the relevant experiment was carried out to evaluate performance of the linear power generator. The principle of the bridge rectifier is shown in Figure 15, two inducing coils A and B were applied in the linear power generator, and six diodes and one capacitor were needed in the bridge rectifier. In the experiment, the vibration excitation was constant, and the output of the proposed rectifier was connected to DAQ board. The MR damper was installed in the MTS which provided the amplitude and frequency excitation. The inducing coils from the generator were connected with the rectifier which adhered with the outer cylinder of the MR damper. In order to prevent the noise signal from DC power source, the DC power source state was set as off. However, there are still large numbers of noises in the experimental data.

Figure 16 shows the inducing voltage of the linear power generator after the rectifier processing. The rectified DC voltage from the two inducing coils is approximately 1.0 V

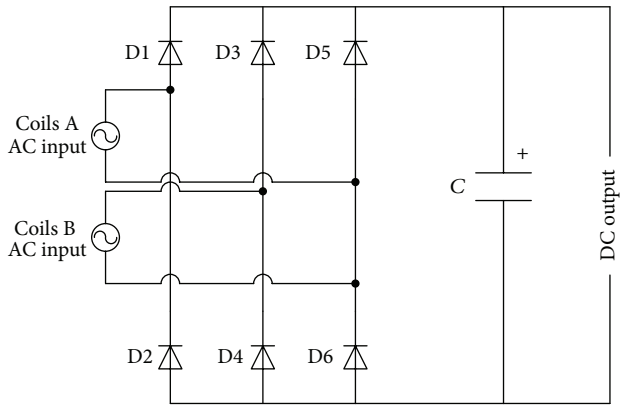

Figure 15: Schematic of the AC-DC rectifier.

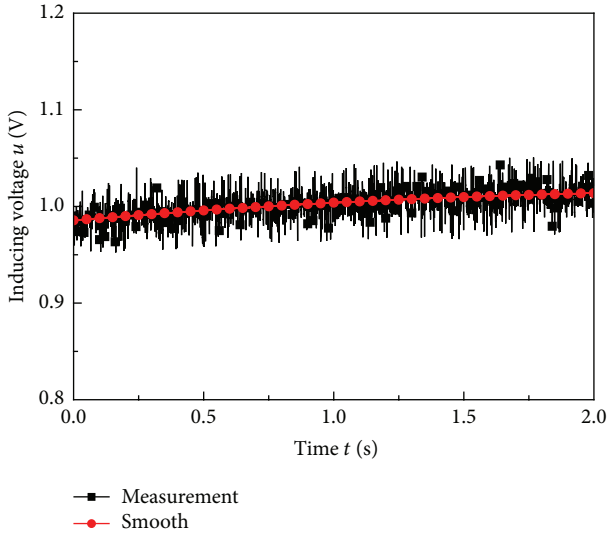

Figure 16: Inducing voltage of linear power generator with AC-DC rectifier.

at 0.06 m·s^{-1} excitation. However, there are still some noises existing in the initial data denoted as black line due to lack of filtering. There are two ways to minimize the signal noises: the first is a commercial rectifier or DAQ board should be adopted as the signal processing unit to minimize the noises from electro circuit. The second is a shield or a filter should be applied to isolate the interference from environment.

5. Conclusions

In this study, an MR damper with energy harvesting ability was designed, fabricated, and tested. The proposed MR damper used the piston rod as the sharing component between the linear power regenerator and the MR damper part, and this shared component could isolate the magnetic field between two function areas. As a result, the magnetic field interference was minimized without extra designed shield and guild layer.

The finite element method was developed to address the magnetic field and magnetic flux distribution of the MR damper part. The simulation result proved the efficiency and feasibility of the proposed MR damper. Then the numerical method was utilized to evaluate the generating performance of the linear power generator, and the finite element model was utilized to investigate the magnetic field distribution. The issue of cogging force and minimization of the magnetic interaction had been solved.

Experimental tests were carried out to address the performances of the proposed MR damper. The results show that the damping force ranges from 200 N at the current of 0 A to 750 N at the current of 0.6 A. The dynamic range equals about 3.75. The AC-DC rectifier was applied on the power generating, and the results show that 1.0 V DC voltage output was harvested after the AC-DC processing.

Competing Interests

The authors declare that there are no competing interests regarding the publication of this paper.

Acknowledgments

This research was financially supported by the National Natural Science Foundation of China (nos. 51475165 and 11462004), the Natural Science Foundation and the Educational Commission Project of Jiangxi Province of China (nos. 20151BAB206035 and GJJ150525), and the Australian Research Council Discovery Project (no. 1501002636).

References

[1] W. H. Li, H. Du, G. Chen, S. H. Yeo, and N. Guo, "Nonlinear viscoelastic properties of MR fluids under large-amplitude-oscillatory-shear," *Rheologica Acta*, vol. 42, no. 3, pp. 280–286, 2003.

[2] X. Zhu, X. Jing, and L. Cheng, "Magnetorheological fluid dampers: a review on structure design and analysis," *Journal of Intelligent Material Systems and Structures*, vol. 23, no. 8, pp. 839–873, 2012.

[3] K. El Majdoub, D. Ghani, F. Giri, and F. Z. Chaoui, "Adaptive semi-active suspension of quarter-vehicle with magnetorheological damper," *Journal of Dynamic Systems, Measurement and Control*, vol. 137, no. 2, Article ID 021010, 2015.

[4] Y. J. Shin, W. H. You, H. M. Hur et al., "Improvement of ride quality of railway vehicle by semiactive secondary suspension system on roller rig using magnetorheological damper," *Advances in Mechanical Engineering*, vol. 6, Article ID 298382, 2014.

[5] H. J. Singh and N. M. Wereley, "Optimal control of gun recoil in direct fire using magnetorheological absorbers," *Smart Materials and Structures*, vol. 23, no. 5, Article ID 055009, 2014.

[6] L. A. Powell, W. Hu, and N. M. Wereley, "Magnetorheological fluid composites synthesized for helicopter landing gear applications," *Journal of Intelligent Material Systems and Structures*, vol. 24, no. 9, pp. 1043–1048, 2013.

[7] K. H. Gudmundsson, F. Jonsdottir, F. Thorsteinsson, and O. Gutfleisch, "An experimental investigation of unimodal and bimodal magnetorheological fluids with an application in prosthetic devices," *Journal of Intelligent Material Systems and Structures*, vol. 22, no. 6, pp. 539–549, 2011.

[8] Q. H. Nguyen, S.-B. Choi, and J. K. Woo, "Optimal design of magnetorheological fluid-based dampers for front-loaded washing machines," *Proceedings of the Institution of Mechanical Engineers, Part C: Journal of Mechanical Engineering Science*, vol. 228, no. 2, pp. 294–306, 2014.

[9] Z. Li, Y.-Q. Ni, H. Dai, and S. Ye, "Viscoelastic plastic continuous physical model of a magnetorheological damper applied in the high speed train," *Science China Technological Sciences*, vol. 56, no. 10, pp. 2433–2446, 2013.

[10] S. Sun, H. Deng, W. Li et al., "Improving the critical speeds of high-speed trains using magnetorheological technology," *Smart Materials and Structures*, vol. 22, no. 11, Article ID 115012, 2013.

[11] G. Yang, B. F. Spencer Jr., H.-J. Jung, and J. D. Carlson, "Dynamic modeling of large-scale magnetorheological damper systems for civil engineering applications," *Journal of Engineering Mechanics*, vol. 130, no. 9, pp. 1107–1114, 2004.

[12] F. Amini and P. Ghaderi, "Optimal locations for MR dampers in civil structures using improved ant colony algorithm," *Optimal Control Applications & Methods*, vol. 33, no. 2, pp. 232–248, 2012.

[13] S. Avadhany, P. Abel, V. Tarasov et al., "Regenerative shock absorber," U.S. Patent No. 8,376,100, February 2013.

[14] S.-B. Choi, M.-S. Seong, and K.-S. Kim, "Vibration control of an electrorheological fluid-based suspension system with an energy regenerative mechanism," *Proceedings of the Institution of Mechanical Engineers, Part D: Journal of Automobile Engineering*, vol. 223, no. 4, pp. 459–469, 2009.

[15] Z. Li, L. Zuo, G. Luhrs, L. Lin, and Y.-X. Qin, "Electromagnetic energy-harvesting shock absorbers: design, modeling, and road tests," *IEEE Transactions on Vehicular Technology*, vol. 62, no. 3, pp. 1065–1074, 2013.

[16] Z. Li, L. Zuo, J. Kuang, and G. Luhrs, "Energy-harvesting shock absorber with a mechanical motion rectifier," *Smart Materials and Structures*, vol. 22, no. 2, Article ID 025008, 2013.

[17] M. Yu, Y. Peng, S. Wang, J. Fu, and S. B. Choi, "A new energy-harvesting device system for wireless sensors, adaptable to on-site monitoring of MR damper motion," *Smart Materials and Structures*, vol. 23, no. 7, Article ID 077002, 2014.

[18] Y. Zhang, K. Huang, F. Yu, Y. Gu, and D. Li, "Experimental verification of energy-regenerative feasibility for an automotive electrical suspension system," in *Proceedings of the IEEE International Conference on Vehicular Electronics and Safety (ICVES '07)*, pp. 1–5, Beijing, China, December 2007.

[19] X. C. Guan, Y. H. Huang, Y. Ru, H. Li, and J. P. Ou, "A novel self-powered MR damper: theoretical and experimental analysis," *Smart Materials and Structures*, vol. 24, no. 10, Article ID 105033, 2015.

[20] S.-W. Cho, H.-J. Jung, and I.-W. Lee, "Smart passive system based on magnetorheological damper," *Smart Materials and Structures*, vol. 14, no. 4, pp. 707–714, 2005.

[21] K.-M. Choi, H.-J. Jung, H.-J. Lee, and S.-W. Cho, "Feasibility study of an MR damper-based smart passive control system employing an electromagnetic induction device," *Smart Materials and Structures*, vol. 16, no. 6, pp. 2323–2329, 2007.

[22] Y.-T. Choi and N. M. Wereley, "Self-powered magnetorheological dampers," *Journal of Vibration and Acoustics, Transactions of the ASME*, vol. 131, no. 4, pp. 0445011–0445015, 2009.

[23] B. Sapiński, "Vibration power generator for a linear MR damper," *Smart Materials and Structures*, vol. 19, no. 10, Article ID 105012, 2010.

[24] B. Sapiński and M. Wegrzynowski, "Experimental setup for testing rotary MR dampers with energy harvesting capability," *Acta Mechanica et Automatica*, vol. 7, no. 4, pp. 241–244, 2013.

[25] B. Sapiński, "Energy-harvesting linear MR damper: prototyping and testing," *Smart Materials and Structures*, vol. 23, no. 3, Article ID 035021, 2014.

[26] C. Chen and W.-H. Liao, "A self-sensing magnetorheological damper with power generation," *Smart Materials and Structures*, vol. 21, no. 2, Article ID 025014, 2012.

[27] B. Ebrahimi, M. B. Khamesee, and M. F. Golnaraghi, "Feasibility study of an electromagnetic shock absorber with position sensing capability," in *Proceedings of the 34th Annual Conference of the IEEE Industrial Electronics Society (IECON '08)*, pp. 2988–2991, Orlando, Fla, USA, November 2008.